Energy-based Multiple-Input-Multiple-Output nonlinear control of fixed-wing aircraft

Leonardo Molino[1], Agostino De Marco[2], and Sabato Manfredi[1]

[1]Università degli Studi di Napoli Federico II,
Dipartimento di Ingegneria Elettrica e delle Tecnologie dell'Informazione (DIETI)[†]

[2]Università degli Studi di Napoli Federico II,
Dipartimento di Ingegneria Industriale (DII)

Abstract. This work introduces a nonlinear control system conceived as a pilot's behavioural model for simulation-based aircraft design workflows. The Total Energy Control System (TECS) technique, a Multiple-Input-Multiple-Output (MIMO) strategy, well represents the pilot's behavioural model in wings-level flight. This study revisits the theoretical foundations of TECS, demonstrating its effectiveness on a fully nonlinear aero-propulsive model of a business jet. TECS manages the aircraft total energy using throttle and elevator, similar to a pilot. The controller has two main blocks: (i) an 'outer loop' control block, vehicle-independent, and (ii) an 'inner loop' control block, specific to the aircraft dynamics. The outer loop uses normalized errors and consistent gains across the flight envelope, while the inner loop is customized to the specific airframe's model, combining local linear controllers into a gain-scheduled nonlinear inner loop controller. This research demonstrates the design and assessment of a nonlinear TECS, ensuring reliable and robust performance across diverse flight scenarios within a realistic, complex nonlinear aircraft representation. The findings highlight this nonlinear control approach, rooted in energy management principles, as a structured framework that emulates pilot behaviour.

Keywords: Flight dynamics, Nonlinear control, TECS, MIMO

1 Introduction

The evolution of aircraft flight control systems reflects the progressive understanding of both longitudinal and lateral-directional dynamics management. In relation to the complexity and computational functions of modern aircraft, these systems can be seen as cyber-physical systems, where real-time data processing and resilience are critical. The traditional design approach treated each control axis (roll, pitch, yaw) independently, following Single-Input-Single-Output (SISO) control architectures [1]. This led to separate control loops for longitudinal and lateral-directional motions, with each axis controlled by a distinct set of actuators and feedback loops.

A significant paradigm shift with respect to the suboptimal multiple SISO-based control techniques began with the recognition that aircraft motion fundamentally represents a coupled, Multiple-Input-Multiple-Output (MIMO) system. In the longitudinal axis, this evolution culminated in the Total Energy Control System (TECS), introduced by Lambregts in the early 1980s [2–4], which represented a fundamental reconceptualization of longitudinal flight control based on energy principles. By explicitly considering the aircraft total energy state and its distribution between potential and kinetic energy, TECS

[†]The contribution of this author is framed within the project "Resilient Optimization in Distributed Cyber-Physical Control Problems subject to Adversarial Behaviour", funded in part by Italian Ministry of University and Research (MUR) within the Progetti di Rilevante Interesse Nazionale (PRIN) 2022 Program under Project 20225MESZB, and in part by European Union - Next Generation EU, Mission 4 Component 2, CUP E53D23000470006.

provides a more natural and efficient approach to coordinated flight path and speed control. Similar advances in lateral-directional control led to the development of the Total Heading Control System (THCS) [5], although energy-based approaches naturally found more application in longitudinal control where potential and kinetic energy exchanges dominate the dynamics.

Traditional flight control systems typically employ separate controllers for altitude and airspeed, leading to potential control coupling issues and suboptimal energy management. The fundamental principle of TECS, that is, the coordinated management of potential and kinetic energy, offers a more elegant solution to these challenges. However, the existing literature predominantly focuses on linearized aircraft models in commercial transport applications. Bruce [6, 7] first implemented TECS on a jet platform. A distinguishing feature of TECS is its fundamental independence from specific aircraft characteristics, stemming from its energy-based formulation [2]. Unlike traditional control architectures that require extensive retuning when applied to different aircraft types, TECS's core algorithm remains largely invariant across platforms. This aircraft independence has been demonstrated through successful implementations across a significant range of aircraft types [8–11]. The energy-based formulation also provides natural handling of nonlinear effects such as thrust lapse with altitude and speed, and variations in lift, drag, and pitching moment characteristics across the flight envelope.

This paper presents an advanced application of TECS to a fully nonlinear model of a business jet aircraft, specifically addressing: (i) the implementation challenges associated to the adaptive elements commonly found in realistic aero-propulsive models, and (ii) the development of a comprehensive flight envelope protection system that leverages TECS's energy-based framework. We introduce some example addressing the requirements of regional transport aircraft, including improved performance during fast departure procedures, and adaptive gain scheduling based on flight condition.

2 Aircraft nonlinear 3-DoF flight dynamics model

The six-degrees-of-freedom (6-DoF) atmospheric motion of a rigid airplane is governed by a system of nonlinear ordinary differential equations [12, 13] embedding a properly engineered aero-propulsive model. The 3-DoF model of an aircraft motion in wings level flight is a particular case of the general 6-DoF formulation. The derivation of such systems assumes a clear identification of two reference frames: a ground-based frame (treated as inertial), and an aircraft-based frame. These two standard reference frames are shown in Figure 1 for the 3-DoF assumption.

From the general formulation provided by De Marco et al. [13] and by Napolitano [14], the full set of equations governing the 3-DoF, longitudinal-symmetric motion of a rigid airplane becomes the following:

$$\dot{u} = \frac{1}{m}\left(W_x + F_x^{(\mathrm{A})} + F_x^{(\mathrm{T})}\right) - q\,w\,, \quad \dot{w} = \frac{1}{m}\left(W_z + F_z^{(\mathrm{A})} + F_z^{(\mathrm{T})}\right) + q\,u \tag{1}$$

$$\dot{q} = \frac{1}{I_{yy}}\left(\mathcal{M}^{(\mathrm{A})} + \mathcal{M}^{(\mathrm{T})}\right) \tag{2}$$

$$\dot{x}_{\mathrm{E},G} = \sqrt{u^2+w^2}\,\cos\left(\theta - \tan^{-1}\frac{w}{u}\right)\,, \quad \dot{z}_{\mathrm{E},G} = -\sqrt{u^2+w^2}\,\sin\left(\theta - \tan^{-1}\frac{w}{u}\right) \tag{3}$$

$$\dot{\theta} = q \tag{4}$$

Equations (1) are known as the Conservation of the total Linear Momentum Equations (CLMEs) [14] — where m is the aircraft mass, and $-m(\dot{u}+qw)$ as well as $-m(\dot{w}-qu)$ are inertial forces. Similarly, Equation (2) is the Conservation of the total Angular Momentum Equation (CAME) in the body frame $\mathcal{F}_\mathrm{B}$ — where the moment of inertia I_{yy} is a known property of the model, $\mathcal{M} = \mathcal{M}^{(\mathrm{A})} + \mathcal{M}^{(\mathrm{T})}$ is the the total, external pitching moment, and $-I_{yy}\dot{q}$ is the inertial couple (see Figure 1). Equations (3) are the Flight Path Equations (FPEs) in the Earth-based inertial frame $\mathcal{F}_\mathrm{E}$, and are used to reconstruct the

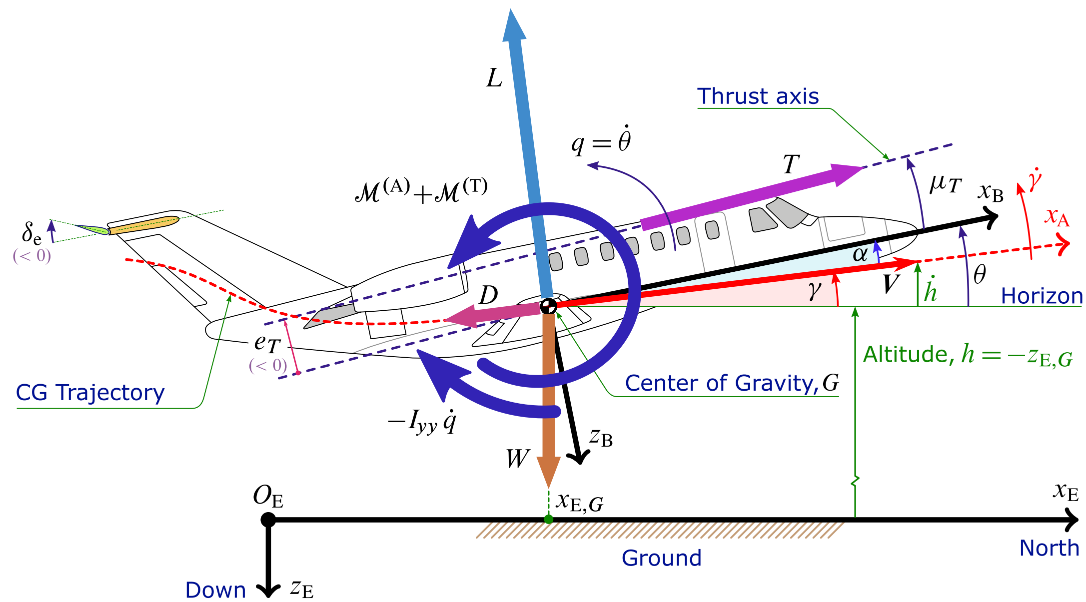

Fig. 1 Earth-based NED frame $\mathcal{F}_\mathrm{E} = \{O_\mathrm{E}; x_\mathrm{E}, y_\mathrm{E}, z_\mathrm{E}\}$ and aircraft body-fixed frame $\mathcal{F}_\mathrm{B} = \{G; x_\mathrm{B}, y_\mathrm{B}, z_\mathrm{B}\}$ in wings level flight (axes y_E and y_B normal to the page). Plane trajectory and velocity vector $\boldsymbol{V}$ of aircraft gravity center G with respect to the inertial observer. Standard definitions of altitude $h = -z_{\mathrm{E},G}$, aircraft second Euler angle θ (Elevation angle), and flight path angle γ. Aerodynamic axis x_A, angle of attack α, elevator angle deflection δ_e, and aerodynamic external actions $(D, L; \mathcal{M})$. Thrust vector, thrust magnitude T, thrust line angle μ_T, thrust line eccentricity e_T.

trajectory of the aircraft gravity center G as a curve in $\mathcal{F}_\mathrm{E}$ — in a 3-DoF and wings level flight, without loss of generality, it is assumed that G moves in the vertical plane $x_\mathrm{E} z_\mathrm{E}$, that remains superimposed to $x_\mathrm{B} z_\mathrm{B}$. Finally, Equation (4) is the 3-DoF rigid-body Kinematic Equation (KE) for the only nonzero aircraft attitude angle θ in wings level flight. It propagates θ in time only in terms of the pitch angular rate q. The reader is referred to the book by Stengel [12] for a comprehensive explanation that justifies the 3-DoF formulation.

As depicted in Figure 1, the aircraft weight $\boldsymbol{W}$ is a vertical force vector, i.e. always aligned to the inertial axis z_E, of magnitude $W = mg$ (with g the gravity acceleration), that is expressed in terms of its components in body-axes: $W_x = -mg \sin\theta$, and $W_z = mg \cos\theta$. The components in body-axes of the instantaneous resultant aerodynamic force are commonly expressed as: $F_x^{(\mathrm{A})} = -D \cos\alpha + L \sin\alpha$, and $F_z^{(\mathrm{A})} = -D \sin\alpha - L \cos\alpha$, where the aerodynamic drag D, and the aerodynamic lift L are involved to conveniently model the effect of the external air flow on the airframe. The state variables (u, w), defined as components in $\mathcal{F}_\mathrm{B}$ of the aircraft gravity center velocity vector $\boldsymbol{V}$, are expressed in terms of α as: $u = V \cos\alpha$, and $w = V \sin\alpha$, where $V = (u^2 + w^2)^{1/2}$ is the instantaneous airspeed. Consequently, the instantaneous angle of attack α is given by $\alpha = \tan^{-1} w/u$. The aerodynamic forces and the aerodynamic pitching moment are expressed in terms of their aerodynamic coefficients according to the conventional formulas: $D = \frac{1}{2}\rho V^2 S C_D$, $L = \frac{1}{2}\rho V^2 S C_D$, and $\mathcal{M}^{(\mathrm{A})} = \frac{1}{2}\rho V^2 S \bar{c} C_\mathcal{M}$, where the external air density ρ is a known function of the flight altitude $h = -z_{\mathrm{E},G}$, S is a constant reference area, $\bar{c}$ is a constant reference chord, and coefficients $(C_D, C_L, C_\mathcal{M})$ are modeled as functions of aircraft state variables, of some state variable rates, and of external inputs.

The resultant thrust force $\boldsymbol{F}^{(\mathrm{T})}$, which is a vector of magnitude T, can be expressed in terms of its body frame components, in the case of symmetric propulsion (zero y-component), as follows:

$F_x^{(\mathrm{T})} = T \cos \mu_{\mathrm{T}}$, and $F_z^{(\mathrm{T})} = -T \sin \mu_{\mathrm{T}}$, where μ_T is a known constant angle formed by the thrust line in the aircraft symmetry plane with the reference axis x_{B}, $T = \delta_T \, T_{\max}(h, M)$, δ_T is the throttle setting (an input to the system), and $T_{\max}(h, M)$ is the maximum available thrust, i.e. a known function of altitude and flight Mach number M. The pitching moment due to thrust is given by the direct action of the thrust vector about the aircraft gravity center, and is expressed as: $\mathcal{M}^{(\mathrm{T})} = T \, e_T$, where the eccentricity e_T is a known parameter, positive when the thrust line is located beneath the center of gravity ($e_T < 0$ as shown in Figure 1).

Equations (1) and (2) are actually set in closed form because all forces and moments are modeled as nonlinear functions of aircraft state variables and external inputs, and commonly as linear functions of some state variable rates. The system of (CLMEs)-(CAMEs)-(FPEs)-(KE), that is (1)-(2)-(3)-(4), is the full set of coupled nonlinear differential equations governing the 3-DoF rigid-body dynamics of atmospheric flight. They propagate the 6-dimensional state vector $\boldsymbol{x} = [u, w, \; q, \; x_{\mathrm{E},G}, z_{\mathrm{E},G}, \; \theta]^{\mathrm{T}}$, while the right-hand sides of (1) and (2) feature the effects of the input vector $\boldsymbol{u} = [\delta_{\mathrm{e}}, \delta_T]^{\mathrm{T}}$, i.e. the elevator deflection angle and the throttle setting δ_T.

A validated high-fidelity, nonlinear aerodynamic and propulsive model for the Cessna Citation II aircraft has been assumed for the case study presented in this work, but the details are omitted here for brevity.

3 The Total Energy Control System (TECS)

As shown also by other works [2, 6, 8] dealing with fixed-wing aircraft configurations, the TECS is a MIMO energy-based navigation control strategy that is capable to provide all vertical flight path and airspeed control mode functions. TECS separates the control loops for flight path and speed, thereby overcoming the limitations of SISO control systems that manage altitude and speed independently. This is accomplished by regulating the aircraft total energy and facilitating energy transfer between acceleration and flight path angle.

Based on the well-known theory of transport aircraft performance [12, 14], where the vehicle is modeled as a point mass, with the further assumption of a slowly varying mass, the total energy of an aircraft in flight can be expressed as the sum $\mathcal{E} = Wh + \frac{1}{2} m V^2$ of its gravitational potential and kinetic energy. Therefore, the specific energy rate $\dot{\mathcal{E}}/(mgV)$ can be expressed as $\dot{E} = \dot{V}/g + \dot{h}/V$.

From the Newton's law applied to the point mass airplane, projected along the instantaneous tangent x_{A} to the flight trajectory, assuming $\theta \approx \gamma$, for small values of the flight path angle [12] — therefore $\sin\gamma \simeq \gamma \Rightarrow \dot{h} = V \sin\gamma \simeq V\gamma \Rightarrow \dot{h}/V \simeq \gamma$, that is, excluding high-performance aircraft such as jet fighters or aerobatic airplanes that can reach high values of θ and γ in climbing flight — it follows that

$$T - D = W\left[\left(\frac{\dot{V}}{g}\right) + \gamma\right] \tag{5}$$

The above expression is known as the 'excess thrust over drag,' also indicated as ΔT.

In level flight ($\gamma = 0$) at constant speed ($\dot{V} = 0$), thrust is trimmed against the drag of the aircraft ($T - D = 0$), so the variation of thrust command with respect to its equilibrium value is defined by

$$\Delta T_{\mathrm{c}} = mg\left(\frac{\varepsilon_{\dot{V}}}{g} + \varepsilon_{\gamma}\right) \propto \varepsilon_{\dot{E}} \tag{6}$$

where $\varepsilon_{\dot{V}} = \dot{V} - \dot{V}_{\mathrm{c}}$, $\varepsilon_{\gamma} = \gamma - \gamma_{\mathrm{c}}$, and $\varepsilon_{\dot{E}} = \dot{E} - \dot{E}_{\mathrm{c}}$ are the errors in $\dot{V}$, γ, and $\dot{E}$, respectively, on the 'commanded' values. According to (6), altering the thrust of the airplane will alter the sum of the airplane flight path angle and acceleration along the flight path, which is proportional to the specific energy rate. Therefore, engine throttle in a fixed-wing aircraft can be used to control the amount of total energy as in a reservoir analogy [3].

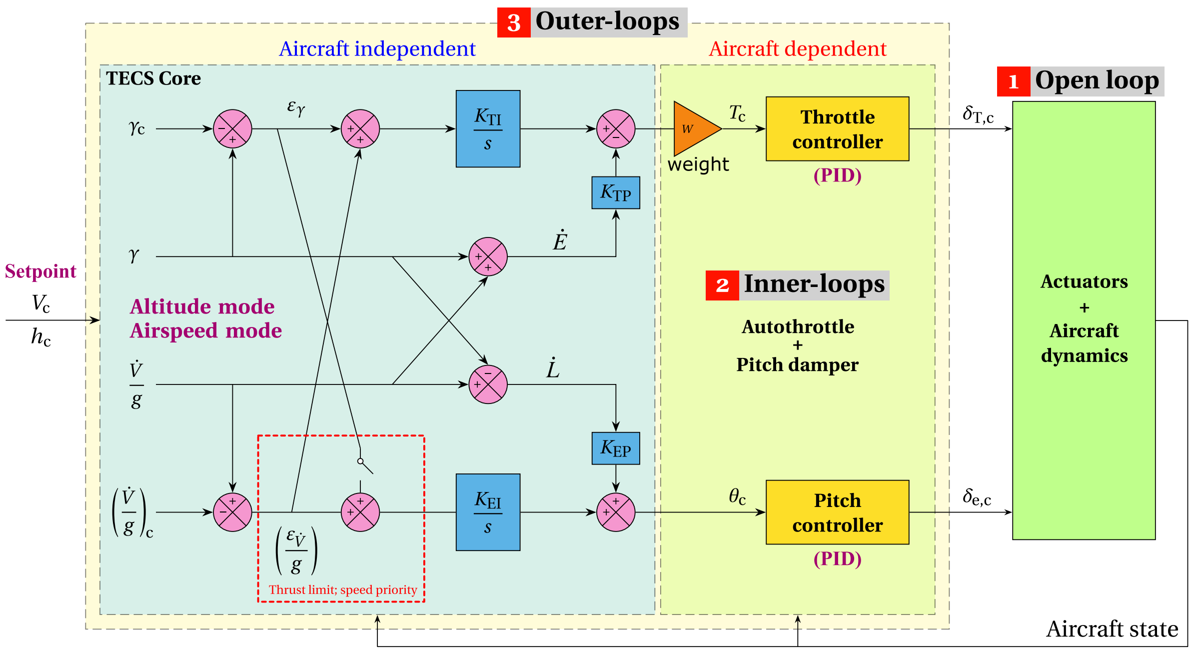

Fig. 2 Autopilot high-level scheme. TECS Core algorithm with speed-priority logic during thrust saturation, as highlighted. Autothrottle and pitch damper inner loops are the aircraft-dependent, gain-scheduled controls.

The TECS Core algorithm structure is illustrated by Figure 2. To generate the control error signals $\varepsilon_{\dot{E}}$ and $\varepsilon_{\dot{L}}$, the (commanded and actual) signals γ_c, γ, $(\dot{V}/g)_c$, and $(\dot{V}/g)$ are required. The chosen control algorithm structure for developing coordinated thrust and elevator commands employs proportional and integral control feedback. However, only $\dot{E}$ and $\dot{L}$ feedbacks are used for the proportional terms instead of the error signals to prevent the creation of unwanted zeros in the system transfer functions, which would lead to undesirable overshoot in the command response.

A simple Proportional-Integral control is then formulated to relate the desired changes in energy rate to thrust (T_c) and thrust setting ($\delta_{T,c}$) commands, in the form of the following transfer laws:

$$T_c = W\left(K_{TP} + \frac{K_{TI}}{s}\right)\varepsilon_{\dot{E}} \implies \delta_{T,c} = \left(K_{\delta_T P} + \frac{K_{\delta_T I}}{s} + K_{\delta_T D}\, s\right) T_c \tag{7}$$

where K_{TP} and K_{TI} are respectively the proportional and the integral gains of the TECS thrust command. According to Figure 2 (Outer-loops, TECS Core), these gains do not depend on the aircraft particular model.

On the contrary, the scheduled gains $K_{\delta_T P}$, $K_{\delta_T I}$, $K_{\delta_T D}$ (Figure 2, Inner-loops, Throttle controller) are the result of thrust control using Proportional-Integral-Derivative (PID) controllers, properly tuned on several linearized plant models. These gains are interpolating functions of airspeed and altitude over sets of fine-tuned values obtained for a dense grid of operating points within the performance envelope of the particular airplane under study. The fine tuning of the aircraft dependent inner-loop thrust control law has been performed with the MATLAB PID tuner app. In this scenario, the integral control (K_{TI}/s) is essential for adjusting T_c to any desired condition and drive the error $\varepsilon_{\dot{E}}$ to zero.

Regarding the other input option to the open-loop plant model, i.e. the commanded elevator $\delta_{e,c}$ deflection, it is well known that elevator control is able to maintain a desired energy level with good approximation [2, 3]. This allows the pilot to exchange potential energy for kinetic energy and vice versa using this aerodynamic surface, without significant short-term energy loss. Therefore, the elevator can be used for energy distribution control. Defining the *specific energy distribution rate*, also known as Lagrangian $\dot{L} = \dot{V}/g - \gamma$, a second Proportional-Integral control law can be applied to convert errors in the desired energy distribution rate $\varepsilon_{\dot{L}}$ into attitude angles and, consequently, into elevator angle commands:

$$\theta_{\mathrm{c}} = \left(K_{\mathrm{EP}} + \frac{K_{\mathrm{EI}}}{s}\right)\varepsilon_{\dot{L}} \implies \delta_{\mathrm{e,c}} = \left(K_{\theta\mathrm{P}} + \frac{K_{\theta\mathrm{I}}}{s} + K_{\theta\mathrm{D}}\, s\right)\theta_{\mathrm{c}} \tag{8}$$

where K_{EP} and K_{EI} are respectively the proportional and the integral TECS core gains of the commanded attitude angle θ_{c}. Again, according to Figure 2 (Inner-loops, Pitch controller), the functions $K_{\theta\mathrm{P}}$, $K_{\theta\mathrm{I}}$, $K_{\theta\mathrm{D}}$ are scheduled PID controllers' gains, that vary according to airspeed and altitude, and are aircraft dependent.

Typically, controlling $\varepsilon_{\dot{L}}$ with the elevator requires an inner-loop control law to stabilize the airplane's short period mode, such as a conventional Stability Augmentation System (SAS)/Control Augmentation System (CAS). The short period SAS/CAS and the engine control loop are the only aircraft-dependent systems in the TECS strategy. They must be designed in a way that they produce similar dynamics, ensuring coordinated control. Moreover, the variable elevator effectiveness must be compensated by gain scheduling the overall elevator command with a set of nonlinear functions of airspeed and altitude.

The TECS core feedback gains K_{TI}, K_{TP}, K_{EI}, and K_{EP} used in developing the thrust and elevator commands, are designed to produce identical dynamics for energy rate error $\varepsilon_{\dot{E}}$ and energy distribution rate error $\varepsilon_{\dot{L}}$, whether for a flight path angle command or a longitudinal acceleration command. The MIMO control law enables precise coordination of thrust and elevator to achieve decoupled command responses. Consequently, a flight path angle command will not cause significant speed deviation and vice versa. Another perspective on command response decoupling is that for a flight path angle or acceleration command, the dynamic response of $\varepsilon_{\dot{E}}$ and $\varepsilon_{\dot{L}}$ must be identical; otherwise, energy is added to or subtracted from the variable intended to remain constant. A typical TECS-based autopilot architecture involves multiple control modes. The one considered here takes two setpoints for the variables V and γ. The error ε_V is converted into an airspeed error signal, which is then multiplied by the factor K_V to get the normalized acceleration command $(\dot{V}/g)_{\mathrm{c}}$. The altitude error is first converted into a vertical speed command by multiplying it with the factor K_h; this vertical speed command is then transformed into a flight path angle command γ_{c} by a division for V_{c}.

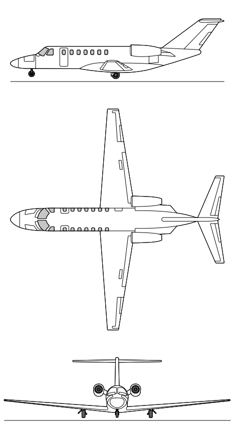

Main properties of the Cessna Citation II aircraft.

Geometric properties	
Length, L	14.54 m
Wing span, b_{W}	15.76 m
Wing surface, S_{W}	29.80 m^2
Wing Aspect Ratio, $\mathcal{R}_{\mathrm{W}}$	8.33
Wing Mean Aerodynamic Chord, $\bar{c}_{\mathrm{W}}$	2.06 m
Longitudinal location of CG, X_G	4.57 m

Weight and balance properties	
Basic Empty Weight, BEW	4073 kg
Maximum Take-Off Weight, MTOW	6713 kg
Maximum Landing Weight, MLW	6123 kg
Maximum Zero Fuel Weight, MZFW	5126 kg
Maximum Fuel Weight, MFW	2204 kg
Empty moment of inertia, $I_{yy,\mathrm{empty}}$	31501 kg m^2
Full moment of inertia, $I_{yy,\mathrm{full}}$	33076 kg m^2

Thrust installation properties	
Thrust line angle, μ_T	2 deg
Thrust line eccentricity, e_T	−1.72 m

Engine operating properties	
Max thrust @ SL, T_{max0}	22.00 kN
Maximum operating Mach, M_{MO}	0.72

Fig. 3 Cessna Citation II aircraft. Three-view drawing and main properties.

4 Nonlinear control simulations for the Cessna Citation II

The Cessna Citation II is a light corporate jet whose three-view drawings and main properties are shown in Figure 3. For a full nonlinear model of this aircraft, the gains of the TECS core algorithm as well as the inner-loop controllers gains (see Figure 2) have been determined in order to meet the following requirements: (i) for a fixed altitude setpoint and a 2 m/s step change of the airspeed setpoint, the altitude should not exceed 1.6 m from its trimmed value; (ii) for a fixed airspeed setpoint and a 10 m step change of the altitude setpoint, the airspeed should not exceed 0.2 m/s from its trimmed value.

Figure 4 shows the results of TECS tuning assessments in terms of time histories of airspeed, altitude, specific energy rates, and commanded inputs. According to the expected TECS decoupling feature, these tests demonstrate that isolated airspeed or altitude changes are achieved with negligible oscillatory altitude or airspeed variations, respectively. The two examples indicate, however, that the control system possesses somewhat slow dynamics. The transfer functions of the open-loop plant (including actuator dynamics) are those of a 5th-order system. Given this complexity, it is not surprising that the presented PI controller is slow in reaching the given setpoints. To address this issue more effectively, a more advanced control strategy such as the Compensator-Prefilter approach would be recommended, but this is beyond the scope of the present work. Yet, it must be noted that this behaviour is acceptable as a guidance approach for the chosen general aviation aircraft.

This study proposes two further testing scenarios of the TECS autopilot design as a pilot behavioural model, achieved by injecting sequences of setpoints on altitude and airspeed (see Figure 2). An aggressive climb simulation has been performed in the next scenario, executing a control task that tracks the maximum rate of Rate of Climb (ROC) performance. This example reproduces a control functionality that can be found in onboard performance management systems. The simulative model incorporates the effects of fuel consumption, reflecting real-world scenarios where mass and inertias are not static but change over time. This refinement enabled a further assessment of the robustness of all controllers. Figure 5 and Figure 6 show the simulation results where the airspeed setpoint has been continuously generated to ensure the aircraft climbing to the target altitude while maintaining the maximum theoretical ROC. This example of a continuously varying setpoint tracking demonstrates an instantaneous fastest and optimal climb, i. e. a minimum-time-to-climb manoeuver.

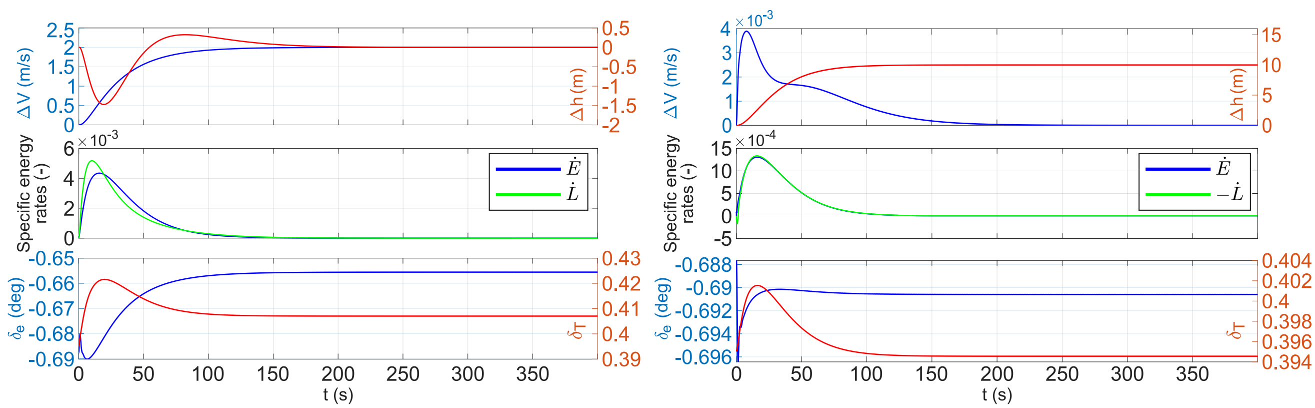

Fig. 4 TECS tuning assessment. Controlled system response to separate step changes in airspeed and altitude setpoints, respectively. The two simulations start from the same initial trimmed flight condition at an altitude of 7000 m and Mach number 0.54. Tuned gains: $K_{\mathrm{TP}} = K_{\mathrm{EP}} = -0.65$, $K_{\mathrm{TI}} = K_{\mathrm{EI}} = 0.20286$, $K_h = K_V = 0.03$. Left: Step demand in airspeed increase of 2 m/s. Right: Step demand in altitude increase of 10 m.

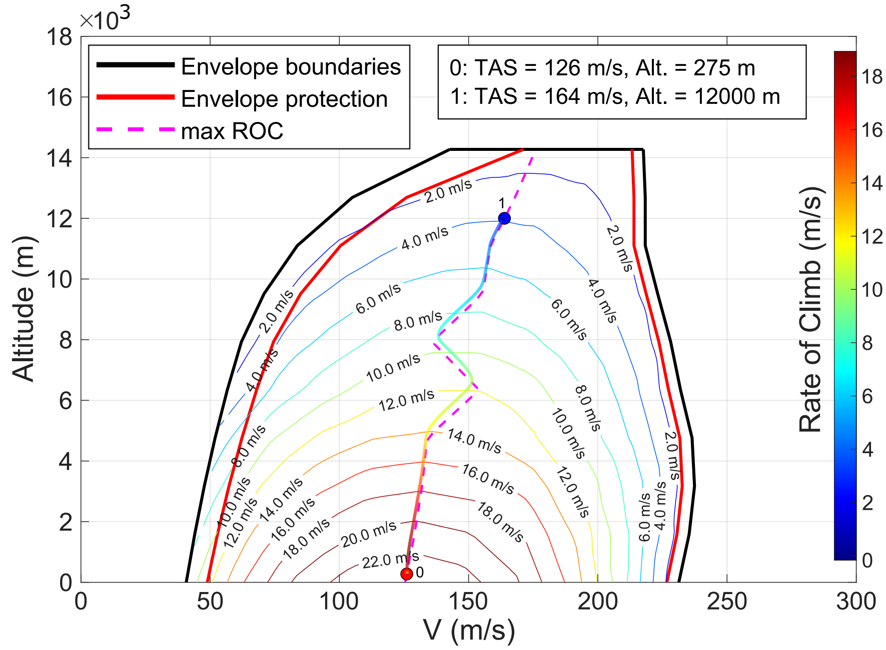

Fig. 5 Flight performance envelope, including ROC time history (coloured line in a climb from Sea Level to an altitude of 12 km) during maximum ROC tracking simulation with varying mass.

Finally, a resilience test is presented to evaluate the robustness of the TECS autopilot design against potential attacks/faults. This test involves injecting an anomalous sequence of altitude and airspeed setpoints, potentially generated by adversarial agents or arising from faults. The simulation results are shown in Figure 7. The aircraft has been instructed to perform: (i) an initial accelerated climb, (ii) a successive steep climb while accelerating, (iii) a descent at constant airspeed, and finally (iv) a steep descent while decelerating. To demonstrate energy management when thrust saturates, an elevator control priority allocation has been performed. During the steep climb segment (ii), the controller saturates the thrust, the commanded flight path angle γ_c goes above the threshold $K_{\mathrm{ECP}}(\gamma + \dot{V}/g)$, hence a Speed-on-Elevator Control Priority (SoECP) is invoked [4]. The gain K_{ECP} defines the amount of energy reserved for climb/descent commands during decelerations/accelerations to select which variable to favour, speed or altitude. The ROC increase in the first two phases (i)-(ii) of the simulation, as the aircraft approaches the airspeed setpoints, is shown in the plot of V. Once the second airspeed setpoint is captured, thrust drops below $T_{\max}$, allowing for smooth capture of altitude. Successively, after the constant speed descent (iii), with the aircraft flying in a steep descent (iv), the commanded thrust reaches its minimum (saturates to zero), and a Path-on-Elevator Control Priority (PoECP) strategy is invoked [4], favouring flight level tracking and limiting the altitude undershoot. The results show that, although under saturation conditions — potentially due to adversarial or anomalous autopilot command signals generated by attacks or faults — the TECS strategy is resilient while still guaranteeing safety and performance.

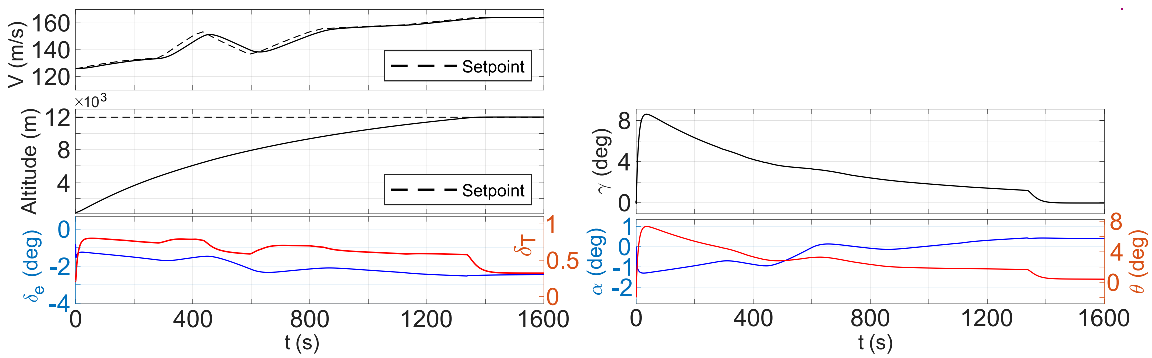

Fig. 6 TECS energy management during maximum ROC tracking simulation with varying mass.

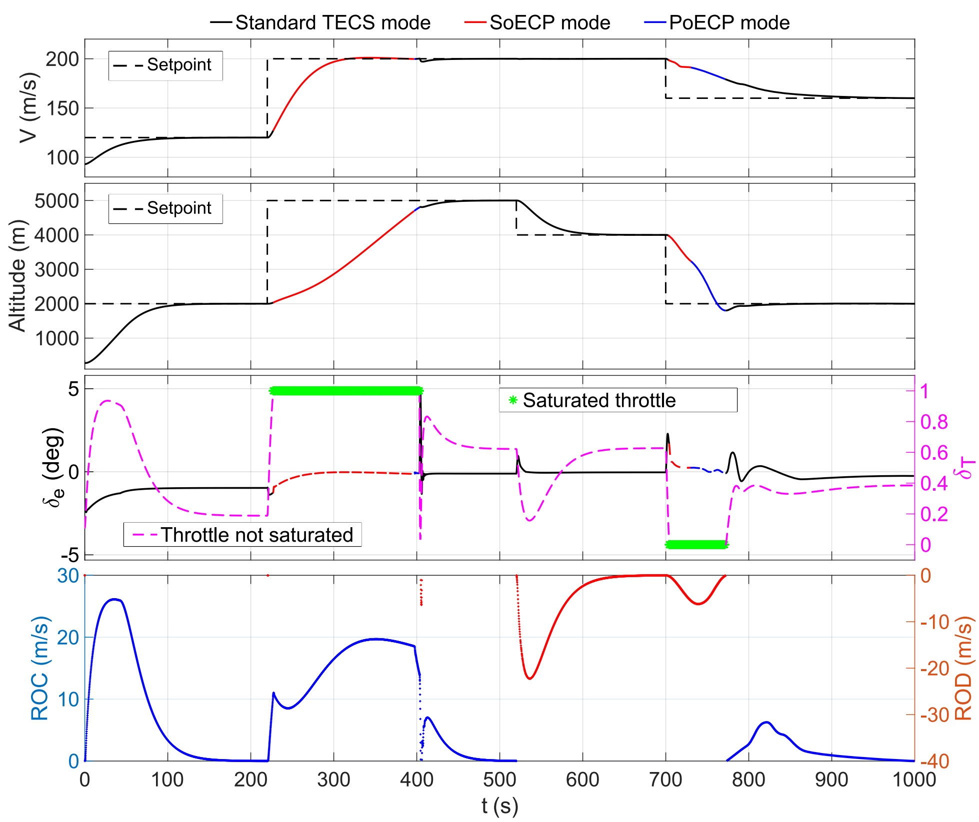

Fig. 7 Elevator control priority switching during the simulation with limit thrust. Thrust saturation is highlighted, as well as special control modes. Rate of descent not saturated and no speedbrakes actuation.

5 Conclusion

This paper presented some selected test cases of TECS applied to a fully nonlinear model of fixed-wing aircraft. The results show that the TECS core algorithm is able to manage the energy states of the aircraft, ensuring coordinated control of thrust and elevator to achieve decoupled command responses. The proposed control strategy is robust and can be used for a wide range of flight conditions, including aggressive manoeuvres and energy management during thrust saturation. The autopilot design is effective in tracking setpoints and maintaining the aircraft within the desired flight envelope. The work demonstrates that this control strategy and its special functioning modes is resilient and can be used as a pilot's behavioural model in simulation-based design workflows.

Acknowledgments – This work has been carried out within the European research project ODE4HERA (project number: 101140510), supported by the Clean Aviation Joint Undertaking and its members.

Disclaimer – Views and opinions expressed are however those of the authors only and do not necessarily reflect those of the European Union or Clean Aviation Joint Undertaking. Neither the European Union nor the granting authority can be held responsible for them.

References

[1] Graham, D., McRuer, D. T. *Analysis of Nonlinear Control Systems*. Wiley, 1961.
[2] Lambregts, A. A. "Vertical Flight Path and Speed Control Autopilot Design Using Total Energy Principles". In: *AIAA Paper* 83-2239 (1983). DOI: 10.2514/6.1983-2239.
[3] Amelink, M., Mulder, M., Van Paassen, M. M., Flach, J. "Theoretical Foundations for a Total Energy-Based Perspective Flight-Path Display". In: *The International Journal of Aviation Psychology* 15 (July 2005), pp. 205–231. DOI: 10.1207/s15327108ijap1503_1.
[4] Lambregts, A. A. "TECS Generalized Airplane Control System Design – An Update". In: *Advances in Aerospace Guidance, Navigation and Control*. Berlin, Heidelberg: Springer Berlin Heidelberg, 2013, pp. 503–534.
[5] Lambregts, A. A. "THCS Generalized Airplane Control System Design". In: *Advances in Aerospace Guidance, Navigation and Control*. 2013.
[6] Bruce, K., Kelly, J., Person JR., L. "NASA B737 flight test results of the Total Energy Control System". In: *Astrodynamics Conference*. American Institute of Aeronautics and Astronautics, Aug. 1986. DOI: 10.2514/6.1986-2143.
[7] Bruce, R. *NASA B737 Flight Test Results of the Total Energy Control System*. Tech. rep. NASA-CR-178285. Boeing Commercial Airplane Company, Jan. 1987.
[8] Faleiro, L., Lambregts, A. "Analysis and tuning of a 'Total Energy Control System' control law using eigenstructure assignment". In: *Aerospace Science and Technology* 3.3 (1999), pp. 127–140. DOI: https://doi.org/10.1016/S1270-9638(99)80037-6.
[9] Shevchenko, A. M. "Energy-based approach for flight control systems design". In: *Automation and Remote Control* 74.3 (2013), pp. 372–384. DOI: 10.1134/S0005117913030041.
[10] Jimenez, P., Lichota, P., Agudelo, D., Rogowski, K. "Experimental Validation of Total Energy Control System for UAVs". In: *Energies* 13.1 (2020). DOI: 10.3390/en13010014.
[11] Chakraborty, I., Mishra, A. A. "Total Energy Based Flight Control System Design for a Lift-Plus-Cruise Urban Air Mobility Concept". In: *AIAA Scitech 2021 Forum*. DOI: 10.2514/6.2021-1899.
[12] Stengel, R. F. *Flight Dynamics*. 2nd ed. Princeton, NJ, USA: Princeton University Press, 2022.
[13] De Marco, A., D'Onza, P., Manfredi, S. "A Deep Reinforcement Learning Control Approach for High-Performance Aircraft". In: *Nonlinear Dynamics* 111.18 (Sept. 2023), pp. 17037–17077. DOI: 10.1007/s11071-023-08725-y.
[14] Napolitano, M. *Aircraft Dynamics: From Modeling to Simulation*. Wiley, 2011.